

A Low-Noise Gain-Enhanced Readout Amplifier for Induced Molecular Electronic Signals

Chung-Lun Hsu^{*}, Tiantian Zhang⁺, Yu-Hwa Lo^{*+}, and Drew A. Hall^{*}

Department of Electrical and Computer Engineering^{*}
University of California San Diego
La Jolla, USA
drewhall@ucsd.edu

Materials Science and Engineering Program⁺
University of California San Diego
La Jolla, USA
ylo@ucsd.edu

Abstract—This paper reports a low-noise readout circuit for label-free, mobile detection of protein-ligand interactions. It is based on a new sensing technique where the surface charge of an electrode is altered due to the dipole moment of nearby biomolecules. We propose a low-noise readout circuit to measure the sub-nA signals. Using a chopped low-noise integrating preamplifier and a resistive transimpedance amplifier, the gain of the proposed circuit is 1.7 G Ω with an input-referred noise of 82 fA_{RMS} over a 10 Hz bandwidth. We demonstrate that the designed amplifier can capture the induced molecular electronic signature of Trypsin with a 50x50 μm^2 sensing electrode.

Keywords—induced molecular electronic signal; chopper stabilization; transimpedance amplifier

I. INTRODUCTION

The detection of protein-ligand binding interaction has been widely studied since characteristics of such interactions, namely the concentration and affinity, are essential in the development and evaluation of new pharmaceuticals. Conventional methods, including Surface Plasmon Resonance (SPR) [1], small molecule microarrays [2], and biologically modified field-effect transistors (BioFET/ChemFET/ISFET) [3], require surface immobilization or fluorescent labeling to detect the protein-ligand binding interaction [3]. Considering the small molecular weight of biomolecules and the importance of unrestricted movement for protein folding, such disturbances imposed by existing techniques can introduce artifacts and produce misleading results. Furthermore, disturbance-free detection is particularly important when molecular engineering is employed to alter the protein or ligand structure to enhance the efficiency and binding kinetics.

Recently, induced molecular electronic signal, a disturbance-free detection method, has been reported to directly observe protein-ligand interactions. As shown in Fig. 1, both the ligand and analyte are free in solution. An induced molecular electronic signature is generated when the net charge at the surface of a sensing electrode is perturbed by the dipole moment or net charge of interacting biomolecules. The amplitude of this signature depends on both the protein/ligand concentration ratio and the specific protein-ligand complex formed. In this application, the background can be controlled to minimize interfering molecules; however, due to the miniscule charge change caused by these small biomolecules, low-noise readout circuitry is crucial to observe this phenomenon.

This work was partially supported by the Hellman Foundation and Vertex Pharmaceuticals, Inc.

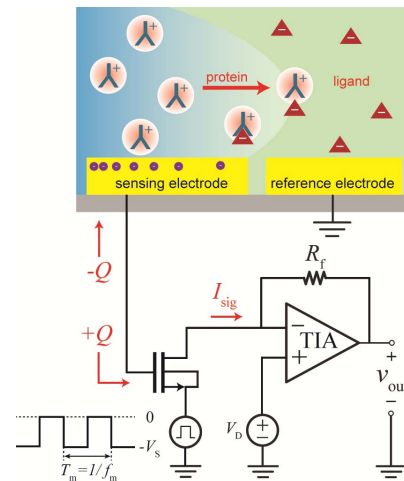


Fig. 1. Principle of the label-free sensing method and low-noise readout circuitry.

The change in charge can be measured using a transimpedance amplifier (TIA), which functions as a current-sensing circuit that converts a current input into a voltage output for further processing and analysis [4-7]. Common implementations include a resistive-feedback TIA (R-TIA) and a capacitive-feedback TIA (C-TIA). However, these traditional implementations suffer from current noise due to the feedback resistor in a R-TIA or kT/C noise from the reset network in a C-TIA as well as flicker noise ($1/f$) and input bias currents from the OPAMP, particularly in discrete implementations, that cause severe loss of signal and degrades the SNR.

In this paper, we present a low-noise, gain-enhanced readout amplifier to measure the biomolecule induced electronic signature from a sensor by cascading a MOSFET with an R-TIA. The MOSFET serves as a low-noise integrating preamplifier to simultaneously enhance the gain of a resistive-feedback TIA and suppress the noise from OPAMP by the unity gain frequency, f_t , of the MOSFET. The MOSFET also functions as a switch for the chopper-stabilization technique to remove the $1/f$ from the circuit without charge injection into the sensor, as in conventional chopping switches. We demonstrate the feasibility of the proposed circuit by measuring protein-ligand interaction with a small 50x50 μm^2 sensing electrode.

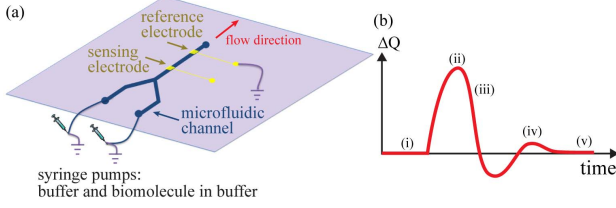


Fig. 2. (a) Illustration of the microfluidic channel for the label-free molecular electronic sensor. (b) Characteristic of the biomolecule signature caused by a biomolecule with a net charge or dipole moment.

II. MOLECULE ELECTRONIC SIGNAL PRINCIPLE AND SENSOR

The label-free molecular electronic sensor is composed of two gold electrodes – a sensing electrode where the reaction is observed and a reference electrode that sets the solution potential. On top of this structure is a microfluidic channel that contains two inlets used to introduce buffer and the biomolecules of interest, and one outlet, as shown in Fig. 2a. Syringe pumps control the flow rate in both channels.

A transient molecular electronic signature is shown in Fig. 2b. When the channel is first filled with an ionic buffer, an equilibrium is established at the solution-electrode interface (i) based on the zeta potential and the double layer capacitance [8]. When a biomolecule flows into the channel and approaches the sensing electrode, the net charge of the sensing electrode is disturbed by dipole moment or charge generating a biomolecular signature (ii). The dipole moment or charge of the biomolecule aligns with the electric field of the sensing electrode, inducing a change in surface charge. Once the shear force due to the laminar flow drives the biomolecule away from the sensing electrode, the net charge decreases (iii). Charge redistribution occurs at the surface of sensing electrode (iv) until the system recovers to a new equilibrium and the net charge changes returns to zero (v). The induced molecular electronic signature depends only on the physical charge interaction at the sensing electrode, rather than on the reaction between the injected and an immobilized biomolecule on the surface of a BioFET [3] or a reduction-oxidation reaction in the channel of a ISFET [8]. Hence, the sensor is more suitable for disturbance-free detection of these interactions.

The amplitude of the electronic signature is proportional to the amount of biomolecule, i.e., the concentration, approaching the sensing electrode. As the protein-ligand interaction occurs, the dipole moment or charge of the complex is altered, thus the amplitude of signal changes. From preliminary measurements, the amplitude is ~ 10 pA for a 1 mM concentration of protein. However, the interaction of two biomolecules generates superimposed signals that are much lower, sub-pA. Therefore, a transimpedance amplifier with input-referred current noise < 1 pA_{RMS} and gain of > 1 G Ω is required to measure molecular electronic signatures. The flow rate is limited by the pressure inside the microfluidic channel, so the duration of the molecular electronic is > 0.1 sec. Hence, the bandwidth requirement of the readout circuit for the molecular electronic is < 10 Hz.

An equivalent circuit model of the sensor in Fig. 2 is shown in Fig. 3. This is a non-faradic process where $C_{u,dl}$ and $R_{u,elect}$ are the unit double layer capacitance and mass transfer resistance of the sensing electrode, respectively; $R_{u,c}$ is the

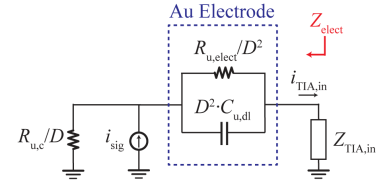


Fig. 3. Circuit model of microfluidic channel and the non-faradiac sensing electrode.

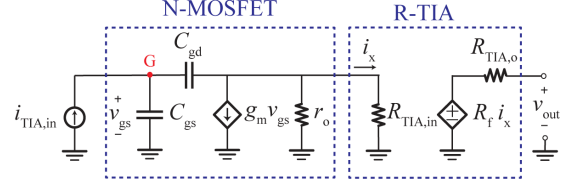


Fig. 4. Equivalent circuit of the proposed low-noise gain-enhanced readout amplifier.

unit channel resistance between the sensing and reference electrode when the distance between electrodes and channel height are fixed while the channel width is designed to be the same as the side length of a sensor; and i_{sig} is the generated signal. In this setup with a channel width of $50 \mu\text{m}$ and an electrode dimension of $50 \times 50 \mu\text{m}^2$, $R_{u,c}$ is ~ 60 G $\Omega/\mu\text{m}$; $C_{u,dl}$ is ~ 1 pF/ μm^2 ; and $R_{u,elect} \sim 10$ G $\Omega \cdot \mu\text{m}^2$ [4, 5].

III. LOW-NOISE GAIN-ENHANCED READOUT AMPLIFIER

A low-noise gain-enhanced readout amplifier with chopper-stabilization is presented to measure these minute molecular electronic signatures. This readout amplifier is implemented as a MOSFET cascaded with an R-TIA, as shown in Fig. 1. Fig. 4 shows the equivalent small-signal model of the readout circuit.

A. Gain

A MOSFET with extremely low gate leakage current is utilized to prevent the loss of signal. When an induced molecular electronic signature is generated, the charge change, ΔQ , at the sensing electrode is transferred to the gate of the transistor due to charge conservation. Note that due to the large channel resistance R_c relative to the impedance $C_{u,dl}$ and $R_{u,elect}$, nearly all of the signal current, i_{sig} is transferred to the TIA. This transferred charge is converted to a voltage, Δv_g , by integrating the charge on the gate capacitance, $C_{g,tot}$:

$$\Delta v_g = \Delta Q / C_{g,tot} \quad (1)$$

The total gate capacitance is $C_{g,tot}$:

$$C_{g,tot} = C_{gs} + C_{gd} \cdot [1 + g_m(r_o \parallel R_{TIA,in})] \approx C_{gs} + C_{gd} \quad (2)$$

where g_m and r_o are the small-signal parameters of the transistor. $C_{g,tot}$ approximately equals the sum of C_{gs} and C_{gd} due to the low input impedance, $R_{TIA,in}$, of the R-TIA. The transistor converts Δv_g to a drain current i_x that is then converted back to a voltage by the R-TIA with a gain of R_f . Hence, the overall gain of the readout amplifier can be derived as:

$$Gain = \frac{v_{out}}{i_{TIA,in}} \approx \frac{g_m}{s(C_{gs} + C_{gd})} R_f = \frac{f_1}{f} \cdot R_f = G_{MOS} \cdot R_f \quad (3)$$

Compared to an R-TIA alone, the gain of the proposed readout amplifier is enhanced by G_{MOS} , i.e., $g_m/s(C_{gs} + C_{gd})$, which is the unity-gain frequency (f_1) of the transistor.

B. Noise

The output impedance of the sensing electrode, Z_{elect} , with a side length of D can be written as:

$$Z_{\text{elect}} = \frac{R_{\text{u,elect}}}{D^2} \parallel \frac{1}{sC_{\text{u,dl}} \cdot D^2} + D \cdot R_{\text{u,c}} \quad (4)$$

The total input-referred current noise of an R-TIA connected directly to the sensor can be derived as [4, 5]:

$$\overline{i_{\text{in,total,R-TIA}}^2} = \overline{i_{\text{n,opamp}}^2} + \frac{\overline{v_{\text{n,opamp}}^2}}{(Z_{\text{elect}} \parallel R_f)^2} + s^2 C_{\text{in}}^2 \overline{v_{\text{n,opamp}}^2} + \frac{4kT \cdot BW}{R_f} \quad (5)$$

where $v_{\text{n,opamp}}$ and $i_{\text{n,opamp}}$ are the input-referred voltage and current noise of the OPAMP, respectively; C_{in} is the total input capacitance of the OPAMP; k is Boltzmann's constant; T is the temperature, and BW is the bandwidth. Note that the noise in a C-TIA is the same as (5) without the term of R_f , so the signal using a C-TIA is also degraded by the noise from OPAMP.

In comparison, the total current noise $i_{\text{drain,total}}$ at the drain of the transistor in the proposed readout amplifier can be derived as:

$$\overline{i_{\text{drain,total}}^2} = 4kT \gamma g_m BW + \overline{i_{\text{n,opamp}}^2} + \frac{\overline{v_{\text{n,opamp}}^2}}{(r_o \parallel R_f)^2} + s^2 C_{\text{in}}^2 \overline{v_{\text{n,opamp}}^2} + \frac{4kT \cdot BW}{R_f} \quad (6)$$

Hence, the total input-referred current noise of the proposed readout amplifier is obtained:

$$\overline{i_{\text{in,total}}^2} = \frac{\overline{v_{\text{in,total}}^2}}{(Z_{\text{elect}} \parallel 1/sC_{\text{gs}})^2} = \frac{1}{(Z_{\text{elect}} \parallel 1/sC_{\text{gs}})^2} \left(\overline{v_{\text{flicker}}^2} + \overline{i_{\text{drain,total}}^2} \right) \quad (7)$$

where the total voltage noise $v_{\text{in,total}}$ at the gate contains the flicker noise v_{flicker} of the MOSFET.

Compared with (5), the noises from OPAMP and feedback resistor R_f are suppressed by both the transconductance of the transistor and the inherent low-pass filtering of the integration in (7), so the total input-referred current noise of the proposed readout amplifier is reduced compared to a conventional R-TIA and C-TIA. The flicker noise from the MOSFET can be ignored due to the major flicker noise is from the sensing electrode [9].

C. Chopping stabilization

Chopping removes the $1/f$ noise from the OPAMP by modulating the low-frequency signal of interest to a higher frequency, away from the $1/f$ noise [10]. In a conventional chopping stabilization circuit, a transistor is used as a chopping switch, and a modulating signal is applied at the gate of this transistor. A sensor and its corresponding readout circuit connect to the source and drain of this transistor respectively. However, the signal from the sensor is degraded by the charge injection from the chopping switches because this extra charge directly superimposes on the signal [4, 5].

In the proposed readout circuit, the MOSFET functions as a low noise amplifier and a switch in the chopping-stabilization technique at the same time. The chopping signal, a square wave with the swing of $-V_S$ to ground, is applied at the source rather than the gate to prevent charge injection from the switch to the sensor. The charge injection of the transistor is

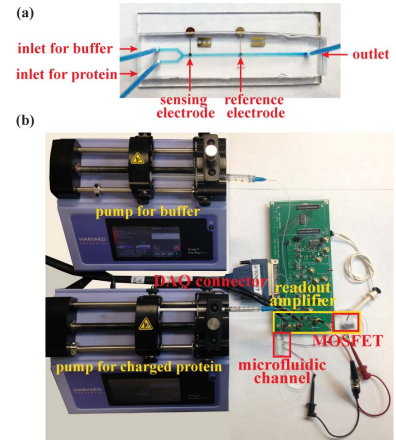


Fig. 5. Photograph of a) fabricated microfluidic channel with electrode size of $500 \times 500 \mu\text{m}^2$, and b) measurement setup showing microfluidic channel and designed low-noise readout circuitry.

suppressed by the transconductance of the transistor. The transistor is simultaneously biased by the chopping signal.

IV. MEASUREMENT SETUP

A. Sensor Fabrication

The microfluidic device was fabricated on a 1 mm thick glass slide. Both the sensing and reference electrodes were deposited with 100 nm titanium (Ti) and 200 nm gold (Au) films using a sputtering system (Denton Discovery 18). The area of the fabricated electrodes are $500 \times 500 \mu\text{m}^2$, $250 \times 250 \mu\text{m}^2$, $100 \times 100 \mu\text{m}^2$, and $50 \times 50 \mu\text{m}^2$, respectively, and the distance between sensing and reference electrode was fixed at 10 mm.

The microfluidic channel was made of polydimethylsiloxane (PDMS) and patterned using a soft lithography (molding) process. The channel width is the same as the side length of corresponding electrode. The PDMS part and the Ti/Au patterned glass slide were aligned and bonded after UV ozone treatment to produce the sensor. The fabricated microfluidic channel is shown in Fig. 5a. The two inlets of microfluidic channel were connected to syringes (BD Plastic) that contained buffer and buffer with dissolved biomolecule, and the flow rates of the syringes were controlled by programmable syringe pumps (Pump 11 elite).

B. Biomolecule Electronic Signal Generation

Trypsin and p -ABA, an enzymatic protein and ligand pair, were reported to generate the molecular electronic signal. Trypsin is a positively charged protein with a strong dipole moment while p -ABA is a molecule with much smaller dipole moment. The amplitude of the signal is increased with the Trypsin- p -ABA complex compared to Trypsin or p -ABA individually. The Trypsin- p -ABA binding process can be characterized by measuring the amplitude increases of the signal. In this paper, a 1 mM Trypsin in 5mM Tris buffer was prepared to generate a fundamental biomolecule electronic signature.

C. Design of low-noise readout amplifier

We verified the concept of the proposed low-noise gain-enhanced readout circuitry and the induced molecular electronic signals using discrete components on a PCB: an enhancement-mode n-type MOSFET transistor (ALD110802),

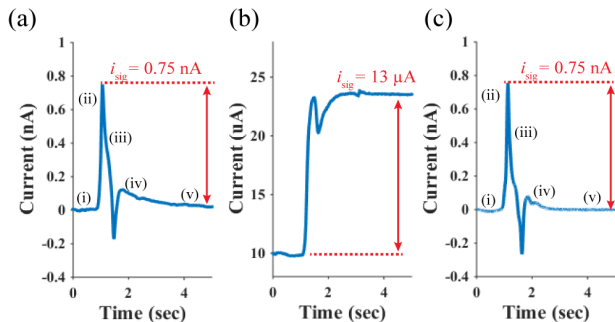


Fig. 6. Measurement results showing biomolecular electronic signature with a $250 \times 250 \mu\text{m}^2$ sensing electrode using (a) an R-TIA with a gain of $200 \text{ M}\Omega$ and (b) the proposed low-noise readout amplifier after demodulation. Differentiating the signal shown in (b) yields a curve in (c).

an OPAMP (OPA627), and a feedback resistor R_f of $100 \text{ k}\Omega$. The requirement of OPAMP are relaxed in terms of noise and input bias current due to the preamplifier. The MOSFET was biased with V_{GS} of 0.4 V and V_{DS} of 5 V for a drain current $\sim 10 \mu\text{A}$. The clock frequency of chopping-stabilization was chosen as 990 Hz to minimize the flicker noise from the transistor and high frequency noise in the third term of (6). A conventional R-TIA with a gain of $200 \text{ M}\Omega$ was also implemented using the same OPAMP for comparison. The output voltage of designed TIA was measured by a data acquisition system, and the chopped signal was demodulated with MATLAB code. Both the setup of microfluidic channel and the designed TIA is shown in Fig 5b.

V. MEASUREMENT RESULTS

Fig. 6 shows the measured biomolecule electronic signatures using both the R-TIA and the proposed amplifier with chopping. The data in Fig. 6a is the input-referred current of the R-TIA and Fig. 6b is the drain current of the MOSFET in our designed readout circuit after demodulating. Due to the charge integration on a gate capacitor as mentioned in (1), the input-referred current in this designed circuit in Fig. 6c was the differentiating result of Fig. 6b. The measurement results also demonstrate that the gain of the MOSFET was $\sim 17 \text{ kA/A}$ from Fig. 6a and b. Therefore, the total gain of readout amplifier is $1.7 \text{ G}\Omega$ using the MOS and the cascaded R-TIA. The curves of signals from measurement results agreed with the theoretical analysis in Fig. 2.

The power spectrum density of the input-referred current noise in both the R-TIA and designed readout amplifier are shown in Fig. 7 measured by a signal analyzer (Agilent 35670A). The integrated input-referred current noise over a bandwidth of 10 Hz is less than $82 \text{ fA}_{\text{rms}}$ in the designed readout amplifier compared to $2.2 \text{ pA}_{\text{rms}}$ for the R-TIA, a $27\times$ reduction using the proposed circuit. The input-referred current noise of the R-TIA was mainly from the OPAMP in this design; while the noise of OPAMP in the readout amplifier, especially the flicker noise, was suppressed by the MOSFET. The signal-to-noise ratio is increased by 47 dB in the designed readout amplifier compared to the R-TIA.

We also characterized the scaling effect of the electrodes. The amplitude of the biomolecule electronic signature depends on the area of sensing electrode because the amount of net charge change is related to the total charge on the electrode surface. The output voltage of the designed readout amplifier is shown in Fig. 8, and we can measure the signal with a sensing

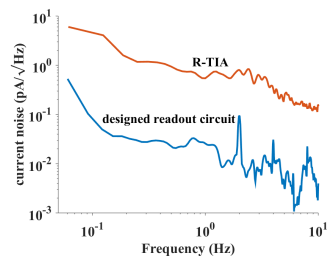


Fig. 7. Measured PSD of input-referred current noise.

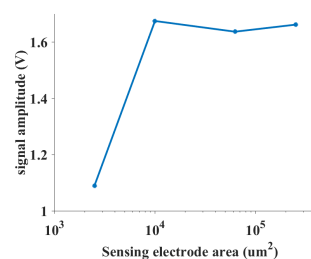


Fig. 8. Measured output signal as a function of electrode size.

electrode as small as $50 \times 50 \mu\text{m}^2$ when the amplitude is less than 10 pA .

VI. CONCLUSION

We report a low-noise gain-enhanced readout amplifier circuit to monitor induced molecular electronic signal for analyzing the protein-ligand interaction without the need of labelling or immobilizing biomolecules on the surface of a sensor. The low-noise readout amplifier with chopping-stabilization technique was proposed to measure the sub-pA biomolecule electronic signal. The signal was enhanced by a MOSFET when this MOSFET served as a low noise amplifier, and the input-referred current noise from the resistive transimpedance amplifier was suppressed at the same time. Biological measurement results demonstrate the feasibility of the proposed readout amplifier for the application of biomolecule electronic biosensor with the sensing electrode of $50 \times 50 \mu\text{m}^2$. The readout amplifier is also a solution for future multichannel integrated sensor chips.

REFERENCES

- [1] B. Liedberg, C. Nylander, and I. Lunström, "Surface plasmon resonance for gas detection and biosensing," *Sensors and Actuators*, vol. 4, pp. 299-304, 1983.
- [2] J. E. Bradner, O. M. McPherson, and A. N. Koehler, "A method for the covalent capture and screening of diverse small molecules in a microarray format," *Nat. Protocols*, vol. 1, pp. 2344-2352, 2006.
- [3] C.-C. Huang and et. al, "AlGaIn/GaN high electron mobility transistors for protein-peptide binding affinity study," *Biosensors and Bioelectronics*, vol. 41, pp. 717-722, 2013.
- [4] K. Dongsoo, B. Goldstein, T. Wei, F. J. Sigworth, and E. Culurciello, "Noise analysis and performance comparison of low current measurement systems for biomedical applications," *IEEE Trans. Biomed. Circuits Syst.*, vol. 7, pp. 52-62, 2013.
- [5] M. Crescentini, M. Bennati, M. Carminati, and M. Tartagni, "Noise Limits of CMOS Current Interfaces for Biosensors: A Review," *IEEE Trans. Biomed. Circuits Syst.*, vol. 8, pp. 278-292, 2014.
- [6] G. Ferrari and M. Sampietro, "Wide bandwidth transimpedance amplifier for extremely high sensitivity continuous measurements," *Review of Scientific Instruments*, vol. 78, p. 7, Sep 2007.
- [7] C. L. Hsu, A. G. Venkatesh, H. Jiang, and D. A. Hall, "A hybrid semi-digital transimpedance amplifier for nanopore-based DNA sequencing," *IEEE Proc. of Biomed. Circuits Syst.*, pp. 452-455, 22-24 Oct. 2014.
- [8] L. M. Shepherd and C. Toumazou, "A biochemical translinear principle with weak inversion ISFETs," *Circuits and Systems I: Regular Papers, IEEE Transactions on*, vol. 52, pp. 2614-2619, 2005.
- [9] E. T. McAdams, et al., "Characterization of gold electrodes in phosphate buffered saline solution by impedance and noise measurements for biological applications," in *IEEE Proc. of Engineering in Medicine and Biology Society*, 2006, pp. 4594-4597.
- [10] H. M. Jafari and R. Genov, "Chopper-Stabilized Bidirectional Current Acquisition Circuits for Electrochemical Amperometric Biosensors," *Circuits and Systems I: Regular Papers, IEEE Transactions on*, vol. 60, pp. 1149-1157, 2013.